Pergamon

Acta mater. Vol. 46, No. 5, pp. 1519–1526, 1998

Printed in Great Britain
PII: S1359-6454(97)00364-9
1359-6454/98 $19.00 + 0.00

ENHANCED HYDROGEN CONCENTRATIONS AHEAD OF ROUNDED NOTCHES AND CRACKS—COMPETITION BETWEEN PLASTIC STRAIN AND HYDROSTATIC STRESS

J. LUFRANO and P. SOFRONIS†

Department of Theoretical and Applied Mechanics, University of Illinois at Urbana-Champaign, Urbana, IL 61801, U.S.A.

(Received 18 March 1997; accepted 6 October 1997)

Abstract—The finite element method was used to solve the coupled elastic–plastic boundary value problem and transient hydrogen diffusion initial boundary value problem. Solutions were obtained at room temperature and under plane strain deformation in the neighborhood of a blunting crack tip under small scale yielding conditions and in the neighborhood of a rounded notch in a four-point bend specimen. The hydrogen population profiles in both normal interstitial lattice sites (NILS) and trapping sites were calculated and conditions for the predominance of the total amount of hydrogen by either of the populations were studied. A discussion of the finite element results in conjunction with different mechanisms of hydrogen embrittlement is presented. If a critical amount of hydrogen is required for hydrogen induced crack initiation, the present results predict locations of crack initiation sites at steel bend specimens which are in agreement with experimental observations on the occurrence of the first microcracking event. © *1998 Acta Metallurgica Inc.*

1. INTRODUCTION

The interaction [1, 2] between solute hydrogen atoms and an applied stress field results from the hydrogen induced volume [3] and local moduli [4, 5] changes that accompany the introduction of the solute hydrogen in the lattice. In regions of tensile hydrostatic stress and softened elastic moduli, interstitial hydrogen has a lower chemical potential [6, 7]. As a consequence, diffusion through normal interstitial lattice sites (NILS) is generated toward these regions tending to eliminate the gradients of the chemical potential. Other transport modes such as through moving dislocations have been considered of negligible effect [8, 9]. Trapping of hydrogen at microstructural defects is an important part of hydrogen embrittlement and its significance lies behind the embrittling mechanisms [10]. The intense plastic straining at the tip of a notch or crack results in high dislocation density. It has been shown that the dislocations in materials trap hydrogen [7, 10–13].

Neglecting trapping at microstructural defects, Van Leeuwen [14] and Hippsley and Briant [15] calculated the solute hydrogen distribution at a crack tip in an isotropic linearly elastic solid under non-steady state conditions of hydrogen transport. Similar calculations of solute hydrogen concentrations in equilibrium with local stresses near a crack tip were done by Liu [16] for an isotropic linearly elastic material and Tong-Yi *et al.* [17, 18] for single crystals of elastically anisotropic iron. Calculations on NILS populations at a crack tip in equilibrium with local stress were recently carried out by Lufrano and Sofronis [19] in the absence of trapping. The effect of trapping on hydrogen transport was first formally modeled by McNabb and Foster [20]. Oriani [21] postulated that at any stage of hydrogen diffusion, the hydrogen population in reversible traps and NILS are in local equilibrium. Based on the Oriani equilibrium model, Sofronis and McMeeking [22] analyzed transient diffusion of hydrogen and hydrogen trapping near a blunting crack tip in iron and steel.

The purpose of this paper is to investigate the competition between tensile hydrostatic stress and traps generated by plastic straining in attracting hydrogen ahead of stress raisers. In particular the aim is to understand and describe quantitatively the conditions under which either of the two competing mechanisms becomes dominant. Possible implications of the corresponding hydrogen population development for hydrogen embrittlement are then discussed.

2. THE HYDROGEN TRANSPORT MODEL IN A MATERIAL UNDERGOING ELASTOPLASTIC STRAINING

Following Sofronis and McMeeking [22], one can assume that hydrogen resides either at normal interstitial sites or reversible trapping sites generated by plastic deformation. The two populations are always in equilibrium according to Oriani theory [21], such that $\theta_T/(1-\theta_T) = K\theta_L/(1-\theta_L)$, where θ_T denotes the occupancy of the trapping

†To whom all correspondence should be addressed.

sites, θ_L denotes the occupancy of the interstitial sites, $K = \exp(W_B/RT)$ represents the equilibrium constant, W_B is the trap binding energy, R is the gas constant equal to 8.31 J/mol·K and T is the absolute temperature. The hydrogen concentration per unit volume in trapping sites, C_T, can be phrased as $C_T = \theta_T \alpha N_T$, where α denotes the number of sites per trap and N_T denotes the trap density measured in number of traps per unit volume. The hydrogen concentration in NILS can be stated as $C_L = \theta_L \beta N_L$, where β denotes the number of NILS per solvent atom and N_L denotes the number of solvent atoms per unit volume. If the available number of trapping sites per unit volume, αN_T, is small compared with the available NILS per unit volume, βN_L, then $N_L = N_A/V_M$, where $N_A = 6.0232 \times 10^{23}$ atoms per mole is Avogadro's number and V_M is the molar volume of the host lattice. The governing equation for transient hydrogen diffusion accounting for trapping and hydrostatic drift is written as [23]

$$\frac{D}{D_{\text{eff}}}\frac{dC_L}{dt} = DC_{L,ii} - \left(\frac{DV_H C_L}{3RT}\sigma_{kk,i}\right)_{,i}, \qquad (1)$$

where $()_{,i} = \partial()/\partial x_i$, d/dt is the time derivative, D is the hydrogen diffusion constant through NILS, D_{eff} is an effective diffusion constant given by $D_{\text{eff}} = D/(1 + \partial C_T/\partial C_L)$, V_H is the partial molar volume of hydrogen in solid solution, σ_{ij} is the Cauchy stress, and the standard summation convention over the range is implied for a repeated index.

The material is assumed to be linearly elastic and isotropic with moduli independent of the local hydrogen concentration. Under plastic straining, it hardens isotropically and flows according to von-Mises J_2 flow theory. The associated flow law is given by the classical Prandtl–Reuss equations. The total deformation rate, $D_{ij} = (v_{i,j} + v_{j,i})/2$, where v_i is the component of the velocity, is expressed as $D_{ij} = D^e_{ij} + D^p_{ij} + D^t_{ij}$ where D^e_{ij} denotes the elastic part, D^p_{ij} is the plastic part, and D^t_{ij} denotes the part due to lattice straining by the solute hydrogen. In the context of the large strain formulation, the hydrogen induced deformation rate, which is purely dilatational [3], is phrased as, $D^t_{ij} = \delta_{ij} d\{\ln[1 + (c\Delta v)/3\Omega]\}/dt$, where c is total hydrogen concentration measured in hydrogen atoms per solvent atom, Δv is the volume change per atom of hydrogen introduced into solution such that $V_H = \Delta v N_A$, Ω is the mean atomic volume of the host metal atom and δ_{ij} is the Kronecher delta.

The hydrogen diffusion initial boundary value problem and the elastic–plastic boundary problem are coupled [22]. The finite element procedures for the solution of the coupled problems are outlined in the work by Sofronis and McMeeking [22] and Lufrano [24]. The formulation of Govindarajan and Aravas [25] for large strain plasticity was adopted to ensure zero lattice strain during large rigid body rotation.

3. HYDROGEN CONCENTRATION PROFILES AHEAD OF ROUNDED NOTCHES AND BLUNTING CRACKS

Sofronis and McMeeking [22] modeled hydrogen transport near a blunting crack for low strength steels, with a yield stress $\sigma_0 = 250$ MPa, a power law hardening exponent, $N = 0.2$, and at temperature 300 K. In their model the trap site density, N_T, increases with plastic straining, ε^p, according to the experimental results of Kumnick and Johnson [11]. A uniform equilibrium hydrogen concentration in the unstressed lattice, $C_0 = 2.084 \times 10^{21}$ atoms per m^3 (2.46×10^{-8} atoms per solvent atom), in equilibrium with gas at one atmosphere pressure was used as an initial condition. The crack was blunted to several times its original opening, under plane strain and small scale yielding conditions.

The results of Sofronis and McMeeking showed that hydrogen accumulates mainly in traps as long as plastic straining generates traps and that the site of accumulation of trapped hydrogen is near the crack surface as dictated by plasticity. When the loading of the crack was just terminated the maximum trapped hydrogen concentration C_T at the crack tip was equal 85.6 times the initial concentration C_0 with trapping site occupancy equal to unity. In contrast, the maximum NILS concentration C_L was only 1.87 as large as C_0 at a distance $R = 1.53b$ from the tip. Once loading was ceased and traps were no longer created by plastic straining, there was little change in the trapped concentration. However, far away from the crack tip, the preponderance of the hydrogen resides in NILS and eventually tends to the equilibrium concentration [6] which can only be elevated by the hydrostatic stress in low strength steels to ≈ 2 times the initial concentration C_0.

Knott [26] points out that the profile of hydrogen distribution may be substantially different in rounded notch specimens in which fractures may occur at stresses below general yield and the plastic strains at the root notch are of the order 5–10% [27]. Knott observes that at these levels of plastic strain, the model of Kumnick and Johnson [11] yields trap densities less than 3.0×10^{21} traps per cubic meter. Therefore the dominant effect of trapping diminishes and the role of the hydrostatic stress may become more significant. Thus, the results of Sofronis and McMeeking [22] should be viewed as an individual case within the range of the dominance regimes to be further explored in this paper.

4. FINITE ELEMENT CALCULATIONS OF THE TRANSIENT HYDROGEN DISTRIBUTION

In this section the competition between the two mechanisms, hydrostatic stress and plastic strain, in attracting hydrogen toward the neighborhood of a crack or a rounded notch at room temperature,

$T = 300$ K, is quantitatively examined. The parameters for both hydrogen diffusion and elastoplasticity were chosen relevant to steel and niobium, as these systems suffer from hydrogen embrittlement, and experimental data are readily available [4, 5, 10].

4.1. Low strength steel: Rounded-notch specimen

The analysis of the rounded notch specimen was carried out using a four-point bend-specimen [27]. A uniform initial NILS concentration of 2.46×10^{-8} atoms per solvent atom was used throughout as an initial condition. The outer surface of the specimen was modeled either as impermeable or was held at constant NILS concentration equal to the initial concentration. The corresponding initial trapping site concentration was calculated, with the parameter α taken equal to 1. The parameter β was set equal to 1 and this corresponds to a maximum NILS concentration of 1 hydrogen atom per solvent lattice atom. The interstitial hydrogen was assumed to expand the lattice isotropically and its partial molar volume in solution was 2.0×10^{-6} m^{-3}/mol [10]. The molar volume of iron was 7.116×10^{-6} m^{-3}/mol and thus $N_L = 8.46 \times 10^{28}$ solvent lattice atoms per m^3. The diffusion constant at 300 K was $D = 1.33 \times 10^{-8}$ m^2/mol [28]. The trap density was calculated as a function of plastic strain according to the experimental findings of Kumnick and Johnson [11]. The Poisson's ratio was 0.3 and Young's modulus was 207 GPa. The extent of deformation in the specimen was measured in terms of a nominal stress defined by $\sigma_{nom} = 6M/wa^2$, where M was the applied bending moment, a was the unnotched ligament and w was the specimen thickness. The nominal stress, σ_{nom}, denotes the maximum bending stress in an straight beam of height a. The specimen was loaded in plane strain by prescribing displacement increments. Three loading tests at constant displacement rates were performed with the displacement increasing linearly with time. Normalized nominal stress, σ_{nom}/σ_0, of 1.0, 2.0 and 3.0 with corresponding equivalent plastic strains of 0.5, 2.0 and 8.0% at the root of the notch developed by the end of loading at time $t_1 = 15$, 35 and 87 s, respectively. The corresponding peak hydrostatic stresses, $\sigma_{kk}/3\sigma_0$, were respectively 1.3, 2.0 and 2.7, and they were achieved, respectively at a distance $R/r_0 = 0.8$, 1.2 and 1.7 from the tip of the notch, where r_0 is the undeformed notch root radius. Subsequently the applied displacements were held constant and hydrogen diffusion continued under fixed external displacement.

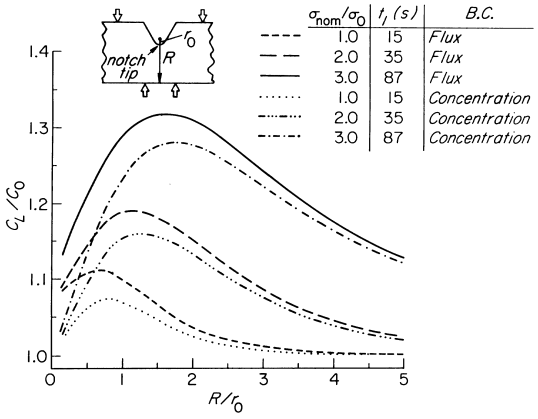

Fig. 1. Plot of hydrogen concentration C_L/C_0 in NILS vs normalized distance R/r_0 from the notch tip in low strength steel ($\sigma_0 = 250$ MPa) at the end of loading at time t_1 with corresponding nominal stress σ_{nom}/σ_0 for both concentration and flux boundary conditions. Initial NILS concentration C_0 equals 2.084×10^{21} hydrogen atoms per m^3.

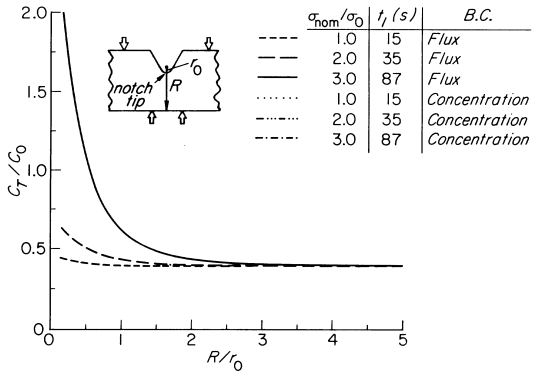

Fig. 2. Plot of hydrogen concentration C_T/C_0 in trapping sites vs normalized distance R/r_0 from the notch tip in low strength steel ($\sigma_0 = 250$ MPa) at the end of loading at time t_1 with corresponding nominal stress σ_{nom}/σ_0 for both concentration and flux boundary conditions.

In the following the hydrogen concentration profiles are plotted vs normalized distance R/r_0 along the symmetry line directly beneath the notch, where R is measured from the tip of the notch. For the three loading courses the normalized hydrogen concentration C_L/C_0, C_T/C_0 and $(C_L + C_T)/C_0$ is plotted in Figs 1–3, respectively, at the end of loading for both flux and concentration boundary conditions. The C_L/C_0 profiles vary with distance from the notch root in accordance with the hydrostatic stress

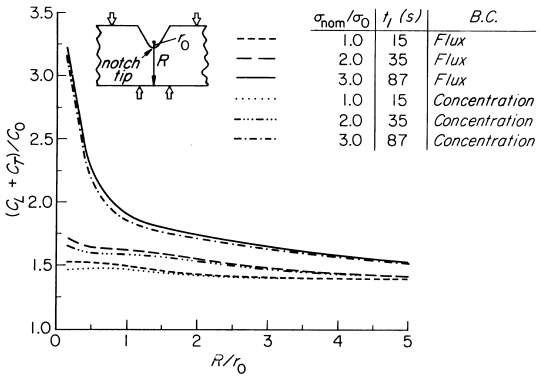

Fig. 3. Plot of total hydrogen concentration $(C_L + C_T)/C_0$ vs normalized distance R/r_0 from the notch tip in low strength steel ($\sigma_0 = 250$ MPa) at the end of loading at time t_1 with corresponding nominal stress σ_{nom}/σ_0 for both concentration and flux boundary conditions.

and the order of magnitude is in accordance with the level of hydrostatic stress elevation. In the case of zero flux boundary condition the NILS concentration is somewhat larger than in the case of constant concentration boundary condition. This is due to the constant egress of hydrogen from the specimen through the notch root in the latter case in order for the concentration to be kept at the constant value of C_0. The C_T/C_0 profiles vary with distance from the notch root in accordance with the equivalent plastic strain. Since the trap binding energy is relatively high, 60 kJ/mol, at room temperature the traps immediately saturate. Only at relatively low plastic strains, i.e. less than 0.5% or equivalently for loads such that $\sigma_{nom}/\sigma_0 \leq 1.0$, is the total hydrogen population in the material dominated by the hydrostatic stress effect, as seen in Fig. 3. At high plastic strains, which occur when $\sigma_{nom}/\sigma_0 > 2.0$, the plastic strain effect dominates. It is notable that this behavior is virtually independent of the boundary conditions.

After the loading terminates and traps are no longer created, the trapped hydrogen concentration C_T/C_0 does not vary with time. However, hydrogen diffusion through NILS continues toward the hydrostatic stress peak location and the local NILS concentration profiles continue to change at all locations until the chemical potential gradients of hydrogen are neutralized. The growth of the hydrogen concentration population and the equilibrium values are shown in Figs 4 and 5 for two different loading cases. For small plastic strains ahead of the notch, $\sigma_{nom}/\sigma_0 \leq 1.0$, the trap concentration is small and the shape of the hydrogen concentration profile depends on the boundary conditions, as seen in Fig. 4. Due to the high binding energy, at room temperature the trapping sites are almost saturated. Accordingly, there is no variation to the trapping concentration due to boundary conditions. Thus the effect of boundary conditions on the total concentration of hydrogen is due to the variations in the NILS concentration. Hence, at low plastic strains,

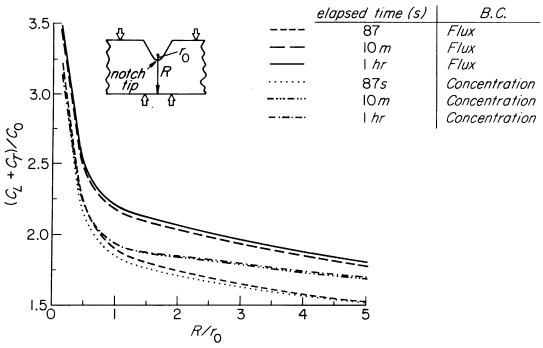

Fig. 5. Plot of total hydrogen concentration $(C_L + C_T)/C_0$ vs normalized distance R/r_0 from the notch tip in low strength steel ($\sigma_0 = 250$ MPa) at three different times during which the nominal stress σ_{nom}/σ_0 was held equal to 3.0 for both concentration and flux boundary conditions.

$\sigma_{nom}/\sigma_0 \leq 1.0$, where the NILS concentration is dominant the boundary condition affects the total hydrogen concentration, as seen in Fig. 4. Whereas, at high plastic strains, $\sigma_{nom}/\sigma_0 > 2.0$, e.g. near general yield where trapping is dominant, the effect of boundary conditions on the total hydrogen concentration is minimal, as seen in Fig. 5.

4.2. High strength steel: Rounded-notch specimen

Since a plastic strain of about 0.5% at the notch surface is a rather small strain in practical applications, additional calculations were carried out in the case of a high strength steel with yield stress $\sigma_0 = 1200$ MPa and $N = 0.2$. As with low strength steel, the problem was solved for the same domain of the rounded notch specimen under external loads applied at a constant displacement rate in time $t_1 = 15$ s and then held fixed. At the end of loading the normalized nominal stress, σ_{nom}/σ_0, was equal to 1.0, the equivalent plastic strain at the tip of the notch was 2.3% and the maximum hydrostatic stress, $\sigma_{kk}/3\sigma_0$, was 2.0 at a distance $R/r_0 = 0.75$ from the tip. The results shown in Fig. 6 indicate that in high strength steels the hydrostatic stress

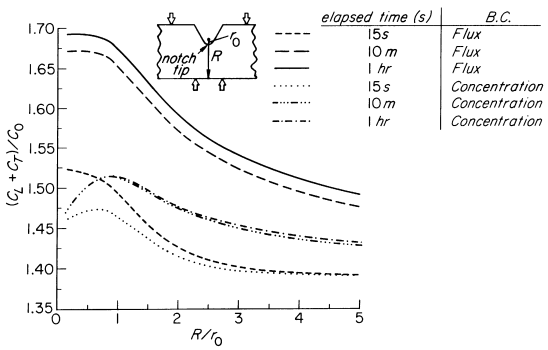

Fig. 4. Plot of total hydrogen concentration $(C_L + C_T)/C_0$ vs normalized distance R/r_0 from the notch tip in low strength steel ($\sigma_0 = 250$ MPa) at three different times during which the nominal stress σ_{nom}/σ_0 was held equal to 1.0 for both concentration and flux boundary conditions.

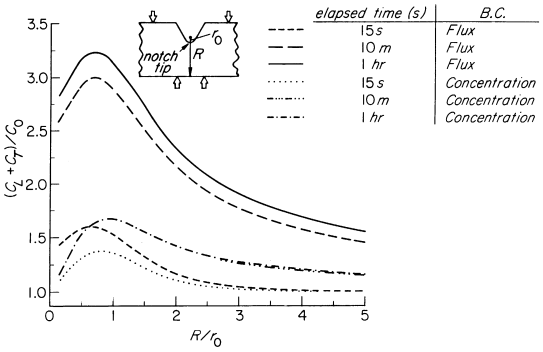

Fig. 6. Plot of total hydrogen concentration $(C_L + C_T)/C_0$ vs normalized distance R/r_0 from the notch tip in high strength steel ($\sigma_0 = 1200$ MPa) at three different times during which the nominal stress σ_{nom}/σ_0 was held equal to 1.0 for both concentration and flux boundary conditions.

dictates the shape of the hydrogen concentration profile even at plastic strains as large as 2.3%. This is due to the large magnitude of the peak hydrostatic stress ($\sigma_{kk}/3$ = 2400 MPa) in comparison with the corresponding small hydrostatic stress ($\sigma_{kk}/3$ = 325 MPa) in low strength steels under the same normalized nominal stress of 1.0.

4.3. Niobium: Blunting crack

The analysis of a blunted crack in a niobium specimen with uniform NILS hydrogen concentration, C_0, was modeled using small scale yielding conditions. As in the case of mild steels both constant concentration, C_0, and zero flux boundary conditions were investigated. Again the parameters α and β were chosen equal to 1. The partial molar volume of hydrogen in solution with bcc niobium was $V_H = 1.88 \times 10^{-6}$ m^3/mol and the expansion of the lattice due to hydrogen was purely dilatational [3]. The molar volume of niobium was 10.852×10^{-6} m^3/mol and the NILS diffusion constant at 300 K was $D = 8.3 \times 10^{-10}$ m^2/s [28]. The trap binding energy was taken 29.2 kJ/mol as has been calculated by Baker and Birnbaum [29]. Since no experimental data for trap populations are available, the trap density was quantified through a dislocation based model for trapping. Assuming that there is one hydrogen atom trapped per atomic plane threaded by a dislocation [30], one finds $N_T = \sqrt{2}\rho/a$, where a is the lattice parameter. The dislocation density, ρ, measured in lines/m^2, was considered to vary linearly with equivalent plastic strain [31], namely $\rho = \rho_0 + \gamma\varepsilon^p$ for $\varepsilon^p < 0.5$ and $\rho = 10^{16}$ for $\varepsilon^p \geq 0.5$, where $\rho_0 = 10^{10}$ lines/m^2 denotes the dislocation density for the annealed material and $\gamma = 2.0 \times 10^{16}$ lines/m^2. Given the lattice parameter $a = 3.3 \times 10^{10}$ m, the maximum number of trapping sites per cubic meter, $\alpha N_T = 4.28 \times 10^{25}$ traps/m^3, was much smaller than the number of the available NILS, $N_L = 5.55 \times 10^{28}$ solvent lattice atoms per m^3. The Poisson's ratio was 0.39 and

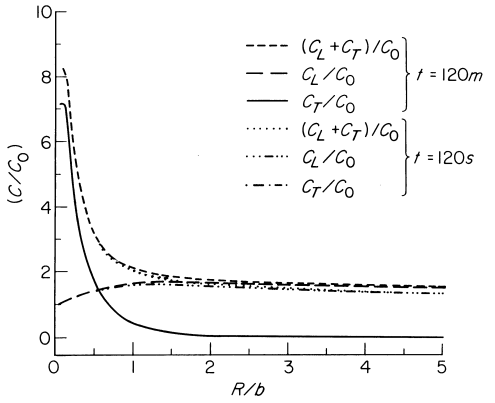

Fig. 7. Plot of hydrogen concentrations vs the normalized distance R/b in front of the crack tip in niobium at times of 120 s and 120 min. The initial NILS concentration equals 10^{-4} H/M.

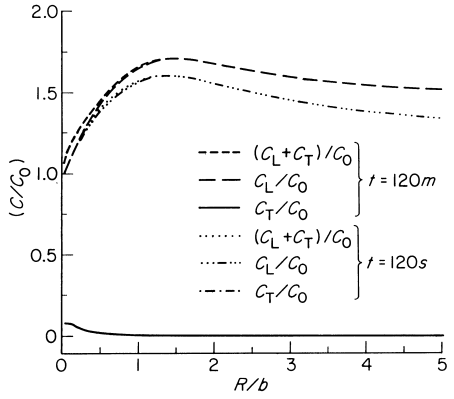

Fig. 8. Plot of hydrogen concentrations vs the normalized distance R/b in front of the crack tip in niobium at times of 120 s and 120 min. The initial NILS concentration equals 10^{-2} H/M.

Young's modulus was 113 GPa. The uniaxial stress –strain law was given by a power-law hardening relationship in which $\sigma_0 = 250$ MPa and N = 0.2. The crack was loaded at a constant displacement rate during a loading time $t_l = 120$ s, at the end of which the final load phrased in terms of the applied stress intensity factor was $K_A = 40$ MPa$\sqrt{\text{m}}$. At times greater than t_l the load was kept constant at $K_A = 40$ MPa$\sqrt{\text{m}}$.

Figures 7 and 8 show the hydrogen concentrations C_L, C_T and the sum $C_L + C_T$ normalized by the initial concentration C_0 plotted against distance R/b on the axis of symmetry ahead of the crack tip when the crack tip opening, b, was equal to three and a half times the undeformed crack tip opening, b_0. The hydrogen concentration profiles are plotted at the end of loading, and after 120 min when hydrogen relaxes to concentration values in equilibrium with local stress. In addition, in Figs 7 and 8 constant concentration C_0 was prescribed as boundary condition over the entire boundary of the specimen. It was found that the results for constant flux boundary condition were not qualitatively different and this is why they are not reported. Figure 7 shows that for an initial concentration of 10^{-4} H/M, i.e. hydrogen atoms per niobium atom, the total concentration is dominated by trapped hydrogen populations and the maximum value is attained close to the crack tip. At this low level of initial lattice concentration, traps are occupied at 92% before straining begins, and this is the reason that no significant change in the trap concentration is observed. After the loading terminates, the changes in the NILS concentration C_L are not significant, an indication that the strain rate is sufficiently slow so that near equilibrium conditions prevail during straining. In calculation with a higher initial concentration, i.e. 10^{-3} H/M, the trap and NILS populations were of the same magnitude at the tip, whereas at distances R/b greater than approximately 0.1 the magnitude of C_L was about 10 times as that

of C_T due to the low plastic strains. As a consequence, a local minimum was observed in the total hydrogen concentration profile in the segment $0 < R/b < 1$. Again no dramatic changes in the transient concentrations were observed and the trap occupancy during straining was always 99%. At an even higher initial concentration, 10^{-2} H/M, the NILS concentrations are much greater than the trap concentrations and the hydrostatic stress dominates the hydrogen distribution at all times, as seen in Fig. 8.

5. DISCUSSION OF THE RESULTS

It has been demonstrated that at room temperature in low fugacity systems, such as irons and low strength steels, hydrogen accumulates mostly in regions of high plastic strain where trapping prevails, unless the plastic strain is very small. Thus in situations of severe plastic straining, as with blunting crack tips or rounded notch specimens with notch root plastic strain greater than ≈2.0%, the total hydrogen concentration, $C_L + C_T$, in the region close to the crack or notch surface is always greater than the concentration at the hydrostatic stress peak location. However, when the plastic strain at the notch root is very small, namely about 0.5%, the calculations show that hydrogen accumulates at the hydrostatic stress peak location in from the tip. At room temperature in a low fugacity and high strength system, such as a high strength steel, even with plastic strains as high as 2.3%, the maximum total hydrogen concentration is at the hydrostatic stress peak and not at the surface of the notch.

In high fugacity systems, such as niobium, the site of accumulation depends strongly on the initial concentration and the magnitude of the plastic strain. At initial concentrations $H/M \leq 10^{-4}$, trapping is dominant and the peak hydrogen concentration, $C_L + C_T$, occurs at the tip of the blunting crack. However, hydrostatic stress dictates the population distribution even in the neighborhood of a blunting crack tip when the initial hydrogen concentration is $H/M \geq 10^{-2}$.

A commonly found assertion in the literature is that a critical hydrogen concentration at some location of the material is needed for the hydrogen embrittling effect to initiate. Thus, if a critical concentration, $C_L + C_T$, alone is the criterion for fracture, one by experimenting with rounded notch bend specimens of low or high strength steels should expect that if fracture occurs at low normalized nominal stresses, ≈1.0, the failure event should first be observed at the hydrostatic stress peak location. The present results on the total hydrogen concentration with the niobium system can be used to verify this thesis by just changing the initial concentration in a cracked specimen. At low concentrations the cracking event should start at the tip whereas at high concentrations the location of the first cracking should be expected to move inside from the tip. Similarly, if a cracked specimen of either low or high strength steel is used and loaded to undergo blunting, the fracture event should be observed first at the tip of the crack. These conclusions are independent of the mechanism responsible for the hydrogen induced failure. Therefore, one cannot identify the type of the mechanism from the cracking location in experiments with cracked and notched bodies if a critical hydrogen concentration is the local fracture criterion. For instance, the mechanism may be lattice decohesion, and the cracking event in a system like niobium may occur under low hydrogen fugacities at a blunting crack tip where the critical concentration condition is first met and the stress is low. On the other hand, the mechanism of embrittlement may be through hydrogen enhanced localized plasticity and the fracture in rounded-notch specimens of low or high strength steel may be first triggered at the hydrostatic stress peak location under loads causing no substantial plastic straining at the tip.

If the criterion for fracture requires a critical concentration, $C_L + C_T$, in combination with a high local stress, say, along the grain boundaries (lattice decohesion) then the experiments on the rounded notch (low or high strength steel) will show cracking in from the tip if fracture occurs at a low nominal normalized stress, ≈1.0. On the other hand a blunted crack specimen of low or high strength steel may not be affected by hydrogen due to absence of high local stresses at the crack tip region despite the presence of high hydrogen concentrations there. In fact, in this case cracking may occur somewhere in between the crack tip and the hydrostatic stress peak location where hydrogen concentration is still far above the initial and the local tensile stress is greater than at the tip location.

If the criterion for fracture requires a critical concentration, $C_L + C_T$, in combination with local material softening (enhanced dislocation motion) then the fracture event in rounded notched specimens of low or high strength steel may not occur until the loads are raised sufficiently high ≈3.0 so that most of the hydrogen is forced to reside close to the highly strained region at the tip where the dislocation density is high. Similarly in a cracked niobium specimen, hydrogen induced cracking may be possible even at low initial concentrations when hydrogen resides mostly close to the tip.

6. IMPLICATIONS FOR HYDROGEN EMBRITTLEMENT IN STEELS

If a critical concentration of hydrogen, $C_L + C_T$, is required for hydrogen embrittlement to occur, the present study can help in rationalizing the location of the first cracking event. However, it should be remembered that the hydrogen concentration predictions are qualitative in nature given

the variability of the model parameters as they apply to a specific steel. For instance, it is not certain whether the Kumnick and Johnson trapping model and the associated binding energy can still be used to the sorts of steels used by other researchers in their experiments. Thus, specific model parameters and pertinent details may first need to be adjusted on a case by case basis to use the present model to reliably determine the hydrogen concentration at the location of the first cracking event.

Lee *et al*. [32, 33] and Onyewenyi and Hirth [34] carried out experiments on precharged rounded notched bend specimens in spheroidized AISI 1095 steel, yield stress of 380 MPa, and spheroidized AISI 1090 steel, yield stress of 345 MPa, respectively. They identified the role of hydrogen as promoting flow localization (plastic instability) [7, 35, 36] that leads directly to crack initiation at the crack surface. The results were independent of the radius of curvature which shows absence of high triaxiality effect. In the experiments of Lee *et al*. [32, 33], void initiation was observed at strains of 6.0% and hydrogen enhanced the formation of deformation induced void initiation. In the experiments of Onyewenyi and Hirth [34], it was found that at strain of 12.0% cracking was demonstrated to occur at the surface of the notch and to begin to propagate along characteristic slip traces before any significant cracking or void formation occurred in the plastically deformed region beneath the notch root. Based on the present numerical study these experiments represent cases of low strength steels in which the total hydrogen concentration close to the surface of the rounded notch is much larger than the concentration away from the surface.

Lee *et al*. [37] performed experiments on precharged U-notched specimens of tempered AISI 4340 steel, $\sigma_0 = 1280$ MPa, and found that the notch root strain for crack initiation was at most 1.0%. They also found that MnS inclusions had little role in the fracture process. The results were interpreted to indicate internal crack nucleation at a critical combination of hydrogen concentration and local stress concentration a result which is consistent with the decohesion theory for hydrogen embrittlement [38–40]. These results pertain to the case modeled in the present calculations in which the total hydrogen concentration in high strength steels under small strains attains its maximum at the hydrostatic stress peak location.

Takeda and McMahon [39] studied the hydrogen effect through tests at notched four-point bend specimens in air and hydrogen using a 5% Ni quenched and tempered steel (based on HY 130). Experimenting on a specimen of yield stress $\sigma_0 = 1060$ MPa, they observed hydrogen induced cracking along shear bands at the notch root and they termed it plasticity related hydrogen induced cracking (PRHIC). It is notable that this PRHIC was observed at high strains prior to specimen failure and in the absence of sufficient impurity segregation. In this case the results of the present numerical study suggest that the preponderance of the hydrogen resides at the notch root when the plasticity is fully developed across the unnotched ligament. On the other hand, a notched specimen of a heat aged 1000 h, $\sigma_0 = 1015$ MPa, microcracked intergranularly at a load less than half of the general yield load in the region between the notch tip and the hydrostatic stress peak location. According to the present study calculations for high strength steels, the location of maximum hydrogen accumulation, $C_L + C_T$, is inside from the notch root at the hydrostatic stress location when the plasticity is limited.

Costa and Thompson [41] investigated the effect of hydrogen on the fracture behavior of a medium-carbon 1045 steel, quenched and tempered at various temperatures. For a tempering temperature of 400°C the yield stress was found to be 1225 MPa, and this allows the use of the results of Fig. 6 in interpreting the hydrogen distribution ahead of the rounded notch in the slow bend tests they conducted on a specimen similar to that of Griffiths and Owen [27]. For this steel, crack initiation took place at such loads as $\sigma_{nom}/\sigma_0 = 2.88$ in the uncharged specimen and $\sigma_{nom}/\sigma_0 = 0.66$ in the presence of hydrogen. At this low level of nominal load, it can be inferred from Fig. 6 that hydrogen should have accumulated at the hydrostatic stress peak location at a distance $R \approx 0.75 r_0$ from the notch root. Costa and Thompson report that the crack initiation event was infrequently identified, because in most cases some propagation of the crack occurred before the loading could be stopped.

In summary, the finite element calculations of the maximum hydrogen accumulation site ahead of a rounded notch subjected to stress are in correspondence with experimental findings on the location of the crack initiation site. When fracture is accompanied by large strains at the notch root, most of the hydrogen is trapped close to the notch root and cracking has been observed to initiate there. In contrast, when limited plastic straining precedes the fracture event most of the hydrogen resides at the NILS sites at the hydrostatic stress peak location inside from the tip. At these occasions hydrogen has been reported to induce microcracking in the highly stressed material volume inside from the notch root.

7. CONCLUSIONS

The numerical results can be summarized as follows:

(i) In four-point bend specimens of low strength steels $\sigma_0 \leq 250$ MPa, NILS populations dominate if the plastic strains at the notch are small (less than 0.5% at $\sigma_{nom}/\sigma_0 \approx 1.0$). At larger strains, trapping populations dominate as in the case of pre-cracked

specimens under small scale yielding conditions [22]. In high strength steels NILS dominance holds at even higher plastic strains at the notch root (≈2.3%, $\sigma_{nom}/\sigma_0 \approx 1.0$). In general, for both low and high strength steels trapped populations dominate when the load is raised to values close and beyond the general yield load.

(ii) In pre-cracked niobium specimens strained under small scale yielding, trapping concentrations dominate at initial concentrations of $H/M \leq 10^{-4}$ and the accumulation site is the crack tip free surface. However, at initial concentrations of H/M 10^{-2} the NILS concentrations dominate resulting in hydrogen concentration profiles ahead of the tip with the local maximum being at the hydrostatic stress peak location.

(iii) In experimental studies with four-point bend specimens, hydrogen induced cracking at the surface of the notch occurred under large strains and microcracking inside from the notch was the case at very small strains. These results, in conjunction with the present numerical calculations of the total hydrogen concentration point to the direction that most of the hydrogen was residing at the microcrack initiation site prior to the onset of fracture. Therefore a critical hydrogen concentration may be a necessary condition for hydrogen embrittlement that merits further investigation.

Acknowledgements—This work was supported by the Department of Energy under grant DEFGO2-91ER45439.

REFERENCES

1. Eshelby, J. D., *Proc. R. Soc. A,* 1957, **241**, 376.
2. Hirth, J. P. and Lothe, J., *Theory of Dislocations*, John Wiley and Sons, New York, 1982, pp. 487–530.
3. Peisl, H., in *Hydrogen in Metals I*, *Topics in Applied Physics*, Vol. 28, ed. G. Alefeld and J. Volkl. Springer-Verlag, New York, 1978, pp. 53–74.
4. Mazzolai, F. M. and Birnbaum, H. K., *J. Phys. F: Met. Phys,* 1985, **15**, 507.
5. Mazzolai, F. M. and Birnbaum, H. K., *J. Phys. F: Met. Phys,* 1985, **15**, 525.
6. Li, J. C. M., Oriani, R. A. and Darken, L. S., *Z. Physik Chem. Neue Folge,* 1966, **49**, 271.
7. Sofronis, P. and Birnbaum, H. K., *J. Mech. Phys. Solids,* 1995, **43**, 49.
8. Ladna, B. and Birnbaum, H. K., *Acta metall.,* 1987, **35**, 1775.
9. Frankel, G. S. and Latanision, R. M., *Metall. Trans. A,* 1986, **17**, 861.
10. Hirth, J. P., *Metall. Trans. A,* 1980, **11**, 861.
11. Kumnick, A. J. and Johnson, H. H., *Acta metall.,* 1980, **28**, 33.
12. Thomas, G. J., in *Hydrogen Effects in Metals*, eds. A. W. Thompson and I. M. Bernstein, *Trans. Met. Soc. AIME*, New York, NY, 1980, pp. 77–85.
13. Angelo, J. E., Moody, N. R. and Baskes, M. I., in *Hydrogen Effects in Materials*, ed. A. W. Thompson and N. R. Moody, *Trans. Met. Soc. AIME.* New York, NY, 1996, pp. 161–170.
14. Van Leeuwen, H. P., *Eng. Fract. Mech.,* 1974, **6**, 141.
15. Hippsley, C. A. and Briant, C. L., *Scr. Met.,* 1985, **19**, 1203.
16. Liu, H. W., *J. Bas. Eng. Trans. ASME,* 1970, **92**, 633.
17. Tong-Yi, Z., Mason, T. A. and Hack, J. E., *Scr. Met.,* 1992, **26**, 139.
18. Tong-Yi, Z., Shen, H. and Hack, J. E., *Scr. Met.,* 1992, **27**, 1605.
19. Lufrano, J. and Sofronis, P., *Int. J. Solids Struct.,* 1996, **33**, 1709.
20. McNabb, A. and Foster, P. K., *Trans. Met. Soc. AIME,* 1963, **227**, 618.
21. Oriani, R. A., *Acta metall.,* 1970, **18**, 147.
22. Sofronis, P. and McMeeking, R. M., *J. Mech. Phys. Solids,* 1989, **37**, 317.
23. Johnson, H. H. and Lin, R. W., in *Hydrogen Effects in Metals*, ed. I. M. Bernstein and A. W. Thompson. Metallurgical Society of AIME, New York, 1981, pp. 3–23.
24. Lufrano, J., *Hydrogen transport in hydride and non-hydride forming metals and the mechanistic implications for fracture behavior*. Ph.D. dissertation, University of Illinois at Urbana-Champaign, Urbana, IL, 1996.
25. Govindarajan, R. M. and Aravas, N., *Int. J. Mech. Sci.,* 1994, **36**, 343.
26. Knott, J. F., in *Hydrogen Effects on Material Behavior*, ed. N. R. Moody and A. W. Thompson, The Minerals, Metals and Materials Society, 1990, pp. 661–675.
27. Griffiths, J. R. and Owen, D. R. J., *J. Mech. Phys. Solids,* 1971, **19**, 419.
28. Volkl, J. and Alefeld, G., in *Hydrogen in Metals I*, *Topics in Applied Physics*, Vol. 28, eds. G. Alefeld and J. Volkl. Springer-Verlag, New York, 1978, pp. 321–348.
29. Baker, C. and Birnbaum, H. K., *Scr. Met.,* 1972, **6**, 851.
30. Tien, J. K., Thompson, A. W., Bernstein, I. M. and Richards, R. J., *Metall. Trans. A,* 1976, **7**, 821.
31. Gilman, J.J., *Micromechanics of Flow in Solids*, McGraw-Hill Book Company, New York, 1969, pp. 185–199.
32. Lee, T. D., Goldenberg, T. and Hirth, J. P., *Metall. Trans. A,* 1979, **10**, 199.
33. Lee, T. D., Goldenberg, T. and Hirth, J. P., in *Fracture 1977*, Vol. 2. University of Waterloo Press, Waterloo, 1977, pp. 243–248.
34. Onyewenyi, O. A. and Hirth, J. P., *Metall. Trans. A,* 1983, **14**, 259.
35. Birnbaum, H. K. and Sofronis, P., *Mater. Sci. Eng. A,* 1994, **176**, 191.
36. Sirois, E. and Birnbaum, H. K., *Acta metall.,* 1992, **40**, 1377.
37. Lee, T. D., Goldenberg, T. and Hirth, J. P., *Metall. Trans. A,* 1979, **10**, 439.
38. Troiano, A. R., *Trans. ASM,* 1960, **52**, 54.
39. Takeda, Y. and McMahon, C. J. Jr., *Metall. Trans. A,* 1981, **12**, 1255.
40. Chen, X., Foecke, T., Lii, M., Katz, Y. and Gerberich, W. W., *Eng. Fract. Mech.,* 1990, **35**, 997.
41. Costa, J. E. and Thompson, A. W., *Metall. Trans. A,* 1981, **12**, 761.